

INFLUENCE OF POLYMETHYLMETHACRYLATE MICROSTRUCTURE ON ITS CONDUCTIVE PROPERTIES AT HIGH TEMPERATURES

Nekane Guarrotxena^{1,} and Miguel Mudarra²*

¹Instituto de Ciencia y Tecnología de Polímeros (ICTP),
Consejo Superior de Investigaciones Científicas (CSIC), Madrid, Spain

²Dept. Física i Enginyeria Nuclear. ETSEIAT,
Universitat Politècnica de Catalunya, Terrassa, Barcelona, Spain

ABSTRACT

The influence of a set of tacticity-governed microstructures on the conductive properties of poly(methyl methacrylate) has been studied at high temperatures. Those structures are specially the mmmr and the mmmrx ($x = m$ or r), which occur when an isotactic sequence breaks-off, and also the rrrm-based termini of syndiotactic sequences. The electrical properties have been studied at the electrical modulus level, assuming a dispersive conductivity to explain conduction processes and Havriliak-Negami equation to evaluate dipolar contribution.

A good agreement between experimental data and the model is observed, and some considerations about the conductive processes can be concluded. Conductivity is thermally activated at the temperature range considered, and ac regime can be associated with a correlated ion hopping of carrier process, which does not reach a strongly correlated regime, what we associate with a high relaxation time of carriers at high temperatures that do allow carriers to follow processes associated to a.c. regime.

Interestingly, conductivity is shown to be dependent on the mmmrm-based stereosequences longer than one heptad. These stereosequences have been shown to exhibit enhanced free volume and rotational motion, what may explain the conductivity-mmmrm structure correlations as found on this work.

Keywords: PMMA, microstructure, tacticity, conductivity, space charge

INTRODUCTION

The objective of this paper is to analyze the influence of a set of tacticity-governed microstructures on the conductive properties of poly(methyl methacrylate) (PMMA). Those

* Corresponding Author E-mail: nekane@ictp.csic.es

structures are specially the mmmr and the mmmrx ($x = m$ or r) which occur necessarily whenever an isotactic sequence breaks-off, and also the rrrm-based termini of syndiotactic sequences. The nature and characterization of all the repeating stereosequences related to tacticity have been widely conveyed in prior work to which the reader is referred [1-7]. A straight relation between these repeating stereosequences and a list of physical properties including dielectrical relaxations, glass transition and electrical space charge nature and distribution, as investigated in our laboratory, has been widely conveyed for PVC and PP polymers [8-20]. Basically, the frequency of those repeating stereosequences, the type of the likely local conformations in some of them, the length of the associated tactic sequences, either iso or syndiotactic, and the atactic parts and the pure mrrm moieties were found to be a major driving force for the inter- and intra-chain interactions and, then, for the physical properties studied.

Such an important correlation was explained to obey the fact that on the one hand microstructures like mmmr, especially when adopting GTTG-TT conformation, exhibit enhanced local free volume and rotational motions, and on the other, the chain alignment and the inter-chain sequential interactions depend on the regularity of the segments separating the former structures [11, 13, 15].

The results enabled us first to assess some original property/microstructure relationships, and second to shed light on the mechanisms of the physical processes involved in most of the polymer behaviors. These mechanisms are of crucial interest in the material science. With the purpose of extending these concepts to other materials of industrial interest, some courses of action concerning PMMA have been endeavored. The first attempt deals with the space charge behavior of three PMMA samples of quite different content and distribution of the above quoted repeating stereosequences, as carefully analyzed by $^1\text{H-NMR}$ spectroscopy. As published recently [21], the straight relation between the nature and amount of space charge and some repeating stereosequences, namely mrrm, rmmr and rrrm, as disclosed in earlier work on PVC and PP samples [13-15, 17], holds well for PMMA, so taking the generalization of that relationship an important step further.

Encouraged by these results we are studying herein the conductive properties of the same PMMA samples, through the dynamic electrical analysis technique. Actually, according to the $^1\text{H-NMR}$ analysis, these polymers present different content of mrrm termini of isotactic sequences of at least one heptad long, located at different intervals of regular chain segments from one sample to another. As a result mrrm, which proved to be traps of negative space charges [13-15, 17] and exhibit favoured rotation facilities, could make the conductivity easy although at different degree for every sample. The same holds, to distinct extents, for the other quoted stereosequences. The study of the electrical conductivity by dynamic electrical analysis will be done at the electrical modulus level [22-24]. A sublinear frequency dispersive ac conductivity has been frequently observed in polymers, so that the real part of the conductivity $\sigma'(\omega)$ can be expressed as:

$$\sigma'(\omega) = \sigma_0 + A\omega^n$$

where σ_0 is the d.c. conductivity, A is a temperature dependent parameter and n is a fractional exponent which ranges between 0 and 1 and has been interpreted by means of many body interactions among charge carriers. This behavior, termed universal dynamic response has been observed in highly disordered materials like ionically conducting glasses, polymers,

amorphous semiconductors and also in doped crystalline solids [25-33]. Equation (1) can be derived from the "universal dielectric response function" [34] for the dielectric loss of materials with free hopping carriers, and this derivation allows one to understand the temperature dependence of parameter A [35].

In the same way, the coupling degree involved in the local motions, as defined by Ngai [36-37], is expected to change from one sample to another. Actually, it was shown to be higher as the rrrm, connected with syndiotactic sequences is more frequent [8-10] and it depends markedly on the conformation in the case of mrrm, where GTTG·TT conformation is much lesser coupled than GTGTTT conformation [8-9]. Interestingly, this coupling is connected with the inter- and intra-chain interactions in that it involves changes in both local free volume and local motion, and it alters the distance between these points and then the length of the regular sequences that are responsible for chain alignments. Therefore the distinct behavior of the samples studied herein should be able to furnish valuable insight into the role of the above stereosequences in the conductive properties of PMMA. Elucidating this relationship is the purpose of the present work.

EXPERIMENTAL SECTION

Materials

PMMA samples (X, Y and Z) provided from commercial source (Atochem) were used in this work. They were purified using tetrahydrofuran (THF, Scharlau) as solvent water as precipitating agent, washed in methanol and dried under vacuum at 40°C for 48 h. THF was distilled under nitrogen with aluminium lithium hydride (Aldrich) to remove peroxides immediately before use.

¹H-NMR Spectroscopy

The tacticity of the three distinct PMMA samples was measured by ¹H-NMR spectroscopy on a Varian UNITY-500 spectrometer operating at 499.88 MHz. Spectra were recorded at 50°C on approximately 10 wt% solutions in deuteriochloroform. Typical parameters for the proton spectra were 8000 Hz spectral width, a 1.9 s pulse repetition rate, 0.5 s delay time and 64 scans. The relative peak intensities were measured from the integrated peak areas, which were calculated with an electronic integrator. The content of the different triads were determined by the electronic integration of the α -methyl signals which appear at (1.3-1.1 ppm), at (1.1-0.9 ppm) and at (0.9-0.7 ppm) corresponding to isotactic (mm), heterotactic (mr) and syndiotactic (rr) triads, respectively [38].

Size Exclusion Chromatography (SEC)

The molecular weight distribution was measured by SEC using a chromatographic system (515 Waters Division Millipore) equipped with a Waters Model 410 refractive index detector. Tetrahydrofuran (THF, Scharlau) was used as the eluent at a flow rate of 1 cm³/min

at 35°C. Styragel packed columns (HR1, HR3, HR4E and HR5E Waters Division Millipore) were used. Poly(methyl methacrylate) standards (PMMA) (Polymer Laboratories, Ltd) in a range between 3.53×10^6 and 5.8×10^2 g/mol were used to calibrate the columns.

The $^1\text{H-NMR}$ data and the molecular weight values are given in Table 1.

Calorimetry

The glass transition temperature (T_g) of the three PMMA samples, performed with a differential scanning calorimeter (DSC), were found equal to 115.6°C, 106°C and 93.5°C for X, Y and Z respectively. About 11 mg of PMMA sample was placed in an aluminium pan and put on a hot plate (170°C, N_2) where it was maintained for 10 min to erase previous thermal history; it was then cooled to 50°C at a fast rate (40°C/min) and a heating DSC run from 50 to 170°C at 2°C/min was carried out.

Dynamic Electric Analysis (DEA)

The real and imaginary parts of the electrical permittivity were measured at several frequencies at isothermal steps of 5°C each. The measurements were carried out using a Novocontrol BDS40 dielectric spectrometer with a Novotherm temperature control system.

The real and imaginary parts of the electric modulus, $M^*(\omega)$, were calculated from the complex permittivity and were fitted to the real and imaginary parts of the electric modulus given by equation (6) simultaneously. Eight independent parameters were used in the fitting process: σ_0 , ω_p , $\varepsilon_{\infty C}$, n , $\varepsilon_{\infty HN}$, τ_{HN} , α and β . The physical meaning of these parameters is introduced later, where equation (6) is derived.

In this work we have used simulated annealing to carry out the fitting process. This method has been successfully used in the analysis of thermally stimulated depolarization currents [39, 40] and dielectric spectroscopy data [41].

RESULTS AND DISCUSSION

Microstructure of the Samples

The $^1\text{H-NMR}$ spectra of samples X, Y and Z are compared in Figure 1. The resonance assignments indicated for the mm, mr and rr centered pentads are those taken from literature [21]. The spectra are typical of predominantly syndiotactic PMMA but showing different isotactic contents. The quantitative amount of mm, mr and rr triads, as measured on the spectra through direct integration of signals, are given in Table 1.

The fractions of the mm, rr, or mr-centered pentads have been determined from the spectra of Figure 1 by deconvoluting the overall triad signals into the individual (or coupled) pentad signals indicated in the Figure 1. It allows both that deconvolution and the distribution of every experimental triad percentage into the corresponding pentad percentages, through an internal mathematical treatment.

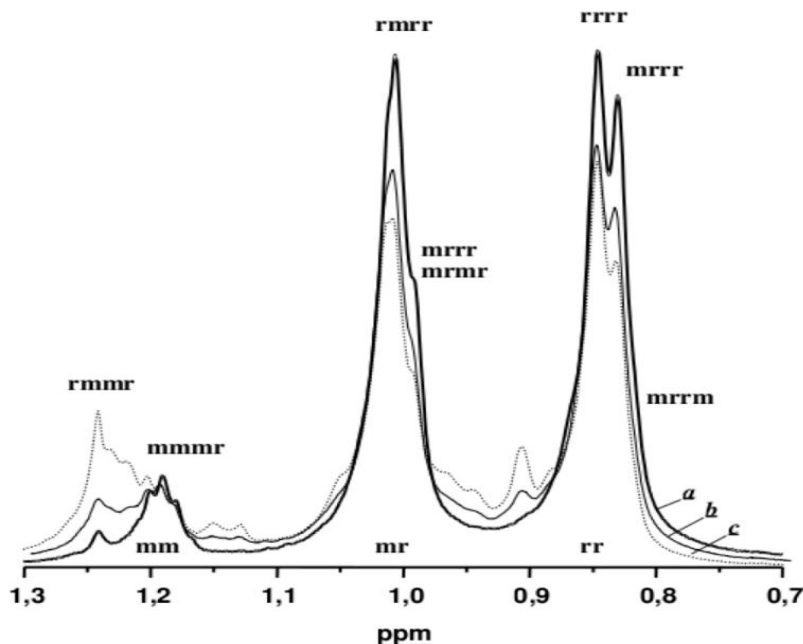


Figure 1. 500 MHz ^1H -NMR spectra of (a) X, (b) Y and (c) Z PMMA samples measured in CDCl_3 at 50°C .

Table 1. ^1H -NMR data for the PMMA samples, ^aPercentage of isotactic (mm), heterotactic (mr) and syndiotactic (rr) triads; ^bPercentage of m ($P_m = \text{mm} + 1/2 \text{mr}$) and rr ($P_r = \text{rr} + 1/2 \text{mr}$) diads

Sample	M_n	mm^a	mr^b	rr^a	P_m^b	P_r^b
X	45500	8.39	43.16	48.45	29.97	70.03
Y	43100	15.16	40.86	43.98	35.59	64.41
Z	44900	20.93	37.92	41.15	38.89	60.11

The data so obtained are shown in Table 2. One way to corroborate their validity is to compare them to the calculated values taking into account the type of repeating sequence statistics, whether Bernoullian or Markovian, of the samples. The extent to which each sample fits into, or departs from, Bernoullian statistics can be determined from the mm, rr and mr & rm triad content as measured on the spectra (Table 1). That quantity is called the persistent ratio and is defined by $\rho = P(s)P(i)/P(is)$, where $P(s) = \text{rr} + 1/2 \text{mr}$; $P(i) = \text{mm} + 1/2 \text{mr}$ and $P(is) = 1/2 \text{mr}$. The results obtained are 0.9725, 1.1220 and 1.2709. These values indicate that sample X is clearly Bernoullian ($\rho = 1$), while samples Y and Z depart somewhat from this statistics. The same was inferred when considering the conditional probabilities of first order Markov statistics [42], another known criteria to examine the type of repeating sequence statistics.

Therefore the pentad fractions were calculated both considering samples Y and Z with Markovian statistics and assuming all the samples as Bernoullian. Interestingly the former values happened to diverge strongly from those measured on the spectra (Table 2), especially in the order of changing from sample X to sample Z. Reversely this order, unlike the absolute values, is quite coincident when considering all the samples as Bernoullian (Table 3). The differences in absolute value are certainly due to the fact that samples Y and Z are only majority Bernoullian. Anyway, what is important for the purpose of this paper are the changes in fraction pentads from one sample to the other, as reflected by Tables 2 and 3.

Table 2. The iso, hetero and syndiotactic pentads values obtained by deconvolution of the triads signals on 1H-NMR spectra of PMMA samples (Figure 1)

Triads	Pentads	Sample		
		X	Y	Z
rr	rrrr	0.395	0.39	0.39
	mrrr+mrrm	0.089	0.049	0.0245
	rmrr+mmrr	0.4197	0.397	0.3070
mr	mrmr+mrrm	0.0118	0.018	0.072
	rmmr	0.019	0.0406	0.0226
mm	mmmr+mmmm	0.064	0.111	0.1866

Table 3. The iso, hetero and syndiotactic pentads values calculated by assuming Bernoullian statistics for PMMA samples

Triads	Pentads	X	Sample	
			Y	Z
rr	rrrr	0.24	0.17	0.13
	mrrr+mrrm	0.4984	0.3474	0.230
	rmrr+mmrr	0.2939	0.295	0.2882
mr	mrmr+mrrm	0.125	0.163	0.191
	rmmr	0.044	0.0525	0.057
mm	mmmr+mmmm	0.0457	0.058	0.0763

Consequently the above results are quite valuable to settle the evolution of any repeating stereosequence from one sample to the other. The sequences that were proved to be the major driving force for the physical properties of PVC and PP according to earlier work, are: i) the average isotactic and syndiotactic sequences length; ii) the mrmr-based and the rrmr-based local structures which occur necessarily whenever an isotactic or syndiotactic sequences

breaks off respectively. Nevertheless, these structures are not active by themselves because it is the occurrence of either one m placement following mmr or one r placement preceding rrm and the length of the $-mm\cdots-$ and $-rrr\cdots-$ sequences connected with them, that were identified as a property determining factor; thence the really important factors are: a) the fraction of mmr followed by one m placement ($-mrrm$ -structures) and the length of the isotactic sequence preceding mrrm. In fact the ratio of $-mrrm$ - repeating stereosequences of at least one heptad in length to the same shorter ones, was proved to be of major importance; and b) the fraction of rrm preceded by one or more r placement, i.e., the $-rrrm$ - structures at the end of syndiotactic sequences; iii) the pure heterotactic $-mrrm$ - sequences and iv) the short atactic moieties like rrrr, mrrr, mrrm and rmmr.

The changes of these repeating stereosequences in X, Y and Z samples can be specified in the light of the above quoted both calculated and experimental results (Tables 2 and 3). It may be thus stated that:

- The average length of isotactic $-mrrm$ - sequences increases from sample X to sample Z and so does the content of mrrm sequence and the length of the isotactic sequence preceding it. As a result the ratio of mrrm stereosequences longer than one heptad to the shorter ones will increase in the order $X < Y < Z$.
- The fraction of $-rrrm$ - structures and the length of the syndiotactic sequence preceding it, will decrease in the order $X > Y > Z$.
- As indicated by the individual calculated values, the fraction of pure heterotactic stereosequences, $-mrrm\cdots-$, hardly changes from one sample to the other. A tiny trend towards decreasing from X to Z is however observed.
- The short atactic moieties, mrrm, rrrr and mrrr decrease in the order $X > Y > Z$, this trend being significant for mrrm only. The rmmr changes in the reverse order.
- On the other hand, it has been extensively conveyed^{1,4} that mrrm can adopt GTTG⁻TT and GTGTTT conformation, the equilibrium between them being strongly displaced towards the latter conformation. It is worthy to note that in PMMA such a displacement should be much enhanced relative to PVC, because of its more hindered rotation facilities. Nevertheless, the occurrence of GTTG⁻TT conformation will decrease in a similar way to mrrm, i.e., $Z > Y > X$.

DEA Measurements

The real and imaginary part of the electric modulus has been plotted as a function of the frequency for several temperatures above the glass transition in Figure 2. Only sample Z case is shown, but similar results can be observed for samples X and Y. In the case of the imaginary part of the modulus, two peaks can be observed in the frequency range studied. The one at higher frequencies is related to molecular motions that results in *alpha* relaxation and the one at lower frequencies is associated with the conductive processes. It can be noted that the peak shifts to higher frequencies with the temperature.

To study the charge transport process at these temperatures we have assumed a sublinear frequency dispersive a.c. conductivity. Power-law dependencies of conductivity, as in the case of equation (1), imply a power-law dependence of the form $(j\omega)^n$ for the complex conductivity [29]. Therefore, this magnitude can be written:

$$(2) \sigma^*(\omega) = \sigma_0 + A(j\omega)^n + j\omega\varepsilon_0\varepsilon_{\infty C}$$

where $\varepsilon_{\infty C}$ refers to the permittivity at high frequency. A crossover frequency ω_p can be defined, $\omega_p = \sigma_0/A$, so that equation (2) can be rewritten as

$$(3) \sigma^* = \sigma_0 + \sigma_0 \left(j \frac{\omega}{\omega_p} \right)^n + j\omega\varepsilon_0\varepsilon_{\infty C}$$

This frequency ω_p is associated with the crossover from the power-law dependence observed at high frequency to a frequency independent d.c. regime that occurs at low frequencies. Finally the contribution to the permittivity is

$$(4) \varepsilon_C^* = -\frac{j\sigma^*}{\varepsilon_0\omega}$$

The alpha relaxation can be modeled by means of Havriliak-Negami equation

$$(5) \varepsilon_{HN}^* = \varepsilon_{\infty HN} + \frac{\Delta\varepsilon}{1+(j\omega\tau_{HN})^{\alpha\beta}}$$

where $\varepsilon_{\infty HN}$ refers to the permittivity at high frequencies and $\Delta\varepsilon = \varepsilon_{\infty C} - \varepsilon_{\infty HN}$ is the relaxation strength. Therefore the electric modulus over the frequency range considered can be expressed as:

$$(6) M^* = (\varepsilon_C^* + \varepsilon_{HN}^*)^{-1}$$

A good agreement between experimental data and values calculated after fitting to equation (6) can be noted in Figure 2, in which σ_0 , ω_p , $\varepsilon_{\infty C}$, n , $\varepsilon_{\infty HN}$, τ_{HN} , α and β were treated as parameters to be fitted.

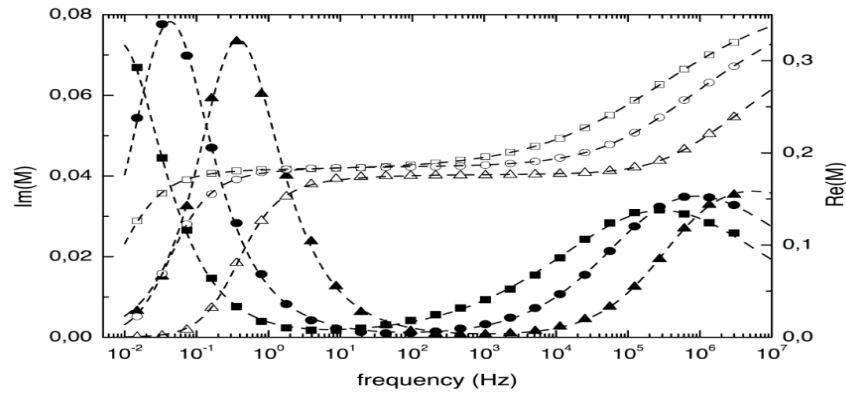


Figure 2. Real and imaginary part of the electric modulus (M) at several temperatures for Z samples. The symbols correspond to experimental values. Lines correspond to values calculated after fitting processes. Im(M): ■ 125°C; ● 140°C; ▲ 160°C. Re(M): □ 125°C; ○ 140°C; △ 160°C.

An Arrhenius plot of the values calculated for the d.c. conductivity σ_0 can be seen in Figure 3. It can be noted that the conductivity is thermally activated in all cases. The values of the preexponential factor σ_{00} and the activation energy E_a in Table 4 indicate that there is a correlation between the content of sequences mrmr and the d.c. conductivity. Indeed, the conductivity is favoured by mrmr structure, that is as the local free volume and rotational motions are enhanced (see NMR analysis, tables and results reported). In fact their content increases from X to Z, so making the mrmr-based stereosequences to be closer what agrees with the observed favored conductivity. The fact that the sequences mrmr equal to or greater than one heptad act as traps for negative carriers, resulting in well-defined space charge profiles observed by Thermal Step supports this hypothesis [21].

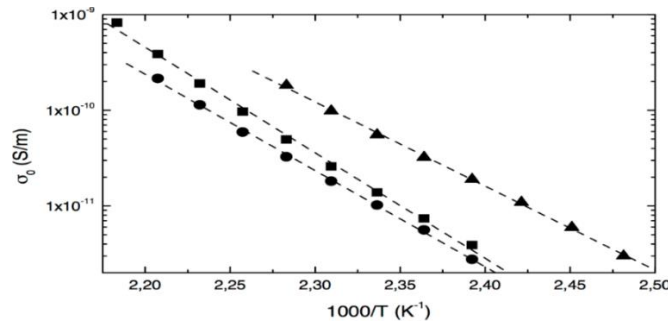


Figure 3. Arrhenius plot of d.c. conductivity σ_0 calculated by fitting equation (6) to data. Samples: ■ X ; ● Y ; ▲ Z.

The temperature dependence of the parameter n is shown in Figure 4. This parameter characterizes the power-law conduction regime, which is associated with the slowing down of the relaxation process in the frequency domain as a result of the cooperative effects, in the same way as the KWW function does in the time domain.

An important connection between these two approaches stems from the coupling model of Ngai and Kannert [43]. This model predicts a power-law conductivity associated with the KWW relaxation function

$$(7) \Phi(T) = \exp[-(t/\tau^*)^\beta]$$

where τ^* is the relaxation time of KWW function. This power law conductivity can be written

$$(8) \sigma_{KWW}(\omega) = \exp(-E_a/kT)\omega^{1-\beta}$$

Table 4. Pre-exponential factor σ_{00} and activation energy E_a resulting from fitting d.c. conductivity σ_{00} to Arrhenius law

Sample	σ_{00} (S/m)	E_a (eV)
X	8.54×10^{14}	2.19
Y	3.35×10^{12}	1.99
Z	2.09×10^{10}	1.75

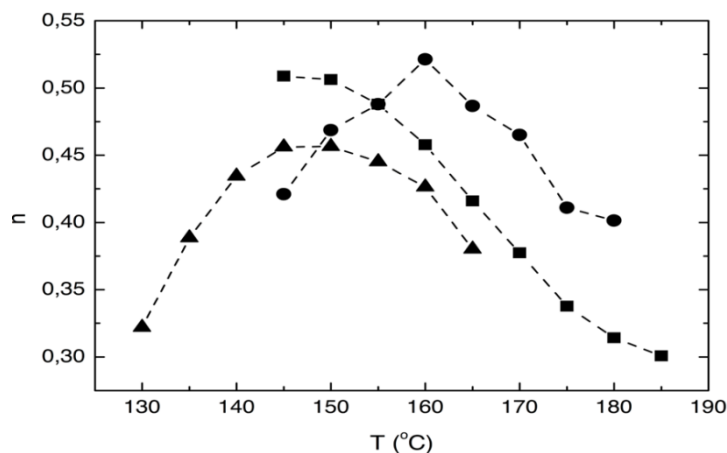


Figure 4. Sublinear power-law exponent n vs. temperature resulting from fitting equation (6) to data. Samples: ■ X ; ● Y ; ▲ Z.

Therefore, if any other contribution is sufficiently smaller than that of σ_{KWW} , then the conductivity of the material may be described by $\sigma_{KWW}(\omega)$ [43]. The sublinear dispersive a.c. conductivity observed in PMMA can be associated with a KWW relaxation mechanism with $\beta=1-n$ where n is the power-law exponent determined from $\sigma(\omega)$.

The stretched exponential parameter β may represent an index of correlation of ionic motion, as the stretched exponential relaxation time has been associated with a slowing of the relaxation process that results from correlated ion hopping, so that one would expect β to be close to zero for strongly correlated systems and close to 1 for random Debye-like hops. As we can see in Figure 4 the power-law exponents in all samples have maxima, at approximately the same temperature (145°C) in the case of samples X and Z, and at 160°C in the case of sample Y. Maxima range between 0.45 and 0.52, indicating that the process does not reach a strongly correlated hopping regime in the temperature range considered.

In all cases, correlation in ion hopping increases initially with temperature, what can be associated with the increase in the carrier concentration, which results in a smaller mean distance and stronger interactions between them. After the maximum, correlation decreases, what we associate with the effect of the increase of local motions of chain segments, which may difficult correlated motions of the carriers.

The above results are in good agreement with those obtained when studying the space charge behavior of the same samples [21] thereby suggesting the role of rrrm- and specially the mrrm-based repeating stereosequences in the conductive properties. The local free volume and rotational motion are different in the later and they could both relate to the nature and frequency of the carriers. In particular the mrrm, contrary to the rrrm, can adopt the GTGTTT or the GTTG $\overline{\text{TT}}$ conformations, of different free volume and rotational motion. The conformational equilibrium $\text{GTGTTT} \rightleftharpoons \text{GTTG}\overline{\text{TT}}$ strongly lies on the left side and is necessarily governed by the temperature. It was demonstrated to work towards the right side at temperatures higher than 120°C [44], what may explain the occurrence of maxima in Figure 4. By comparing the properties behavior of samples of different content of mrrm- and rrrm- based stereosequences, those processes were argued to be accompanied by changes in parameter n and, consequently, in local or sequential chain correlations [21]. It was thus

concluded the outstanding role of those stereosequences in a set of physical properties of polymer materials [8-21]. The changes in conductive properties obtained herein clearly suggest the same type of correlation. The apparent deviation of sample Y in Figure 4 is presumably due to the offsetting effects of rrrm- and mrrm- based sequences which are both intermediate magnitude between those of X and Z samples.

Figure 5 shows the correlation between Maxwell relaxation time

$$(9) \tau_M = \frac{\varepsilon_0 \varepsilon_r}{\sigma_0}$$

which characterizes the charge carrier relaxation process and the characteristic time

$$(10) \tau_p = \frac{2\pi}{\omega_p}$$

that determines the transition from d.c. regime to a.c. regime. In the case of low temperatures it seems that both times take the same value (in Figure 5 a dashed line indicates, $\tau_M = \tau_p$). At higher temperatures both times decrease with temperature, as it is expected, but Maxwell time, associated with carrier mobility is higher than the time that characterizes the regime transition (Maxwell time decreases at a lower rate). This indicates that carrier relaxation time is larger than the characteristic time of the processes involved in a.c. regime. This may be the reason of the decreasing of the carrier motion correlation with the temperature: time that determines carrier mobility is too high to allow carriers to follow processes associated to a.c. regime at high temperatures.

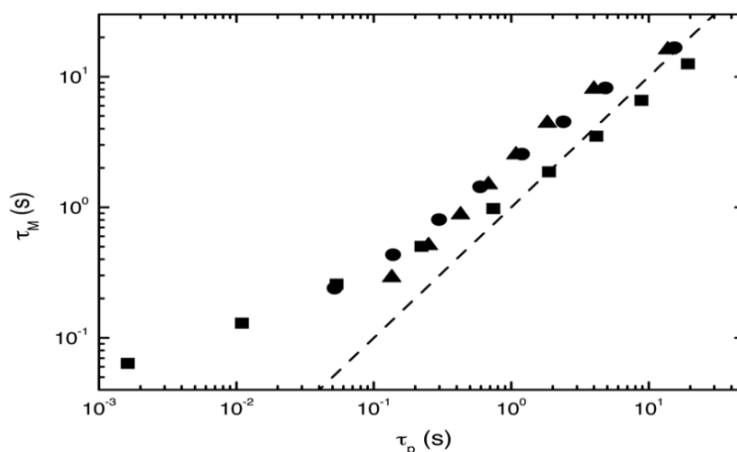


Figure 5. Correlation between Maxwell relaxation time τ_M and the characteristic time (τ_p) that determines the transition from d.c. regime to a.c. regime. Samples: ■ X ; ● Y ; ▲ Z. Dashed line is a guide to the eye to indicate $\tau_p = \tau_M$.

In the case of the maximum values of n in each case, it can be seen that samples X and Y reach similar values, which are higher than in the case of sample Z. This result agrees with the explanation given above for d.c. conductivity. There is also a correlation between the content of mrrm-based sequences and the parameter n and it relates both to the overall

content of the latter sequences and to the conformational equilibrium $\text{GTGTTT} \rightleftharpoons \text{GTTG}\cdot\text{TT}$ between the conformations which are likely in them. These structures condition the presence of regions with larger free volume and enhanced local rotational motions in regularly spaced locations of the chain, thereby influencing the chain correlations [21] and then the conductive properties.

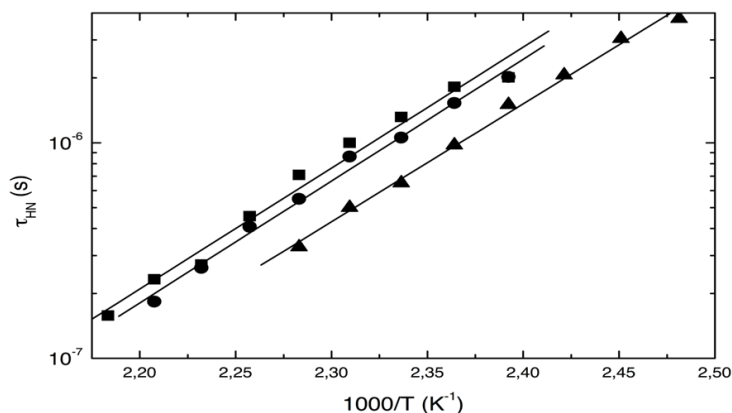


Figure 6. Arrhenius plot of relaxation time in Havriliak-Negami equation (τ_{HN}) resulting from fitting equation (6) to data. Samples: ■ X ; ● Y ; ▲ Z.

Table 5. Pre-exponential factor τ_{HNO} and activation energy E_a resulting from fitting relaxation time to Arrhenius law

Sample	τ_{HNO} (s)	E_a (eV)
X	9.44×10^{-20}	1.11
Y	6.67×10^{-20}	1.12
Z	1.11×10^{-19}	1.08

The relaxation time in Havriliak-Negami equation has been represented in an Arrhenius plot (Figure 6). Havriliak-Negami equation has been used to model the relaxation observed at the high frequency range observed in our measurements (Figure 2). This relaxation is associated with the cooperative motions of chain segments which are allowed above the glass transition. The temperature range of the experiments is somewhat above the glass transition temperature of each of the samples (T_g values can be seen in the experimental section). At these temperatures there are not volume restriction and we can see that kinetics obeys Arrhenius law. The values of the pre-exponential factors and activation energies corresponding to the samples used can be seen in Table 5.

As can be seen, the correlation between both magnitudes with the GTTG·TT content is quite apparent, even if sample Y exhibits some deviation because of the above mentioned offsetting effects of rrrm- and mrrm- sequences relative to X and Z samples. Indeed, the predominance of either rrrm or mrrm stereosequences is much more marked in samples X or Z respectively.

CONCLUSION

The influence of microstructure on the conductive properties of Poly(methyl methacrylate) has been studied at high temperatures. The electrical properties have been studied at the electrical modulus level, assuming a dispersive conductivity to explain conduction processes and Havriliak-Negami equation to evaluate dipolar contribution with a good agreement between experimental data and the model.

Conductivity is thermally activated at the temperature range considered, and a.c. regime can be associated with a correlated ion hopping of carrier process, which does not reach a strongly correlated regime. We associate the initial increase in the correlation with the increase of carrier concentration.

Conductivity is concluded to be favored by mrrm-based stereosequences longer than one heptad. According to prior work [21] the latter exhibit enhanced local free volume and rotational motion, what would involve significant changes in carriers correlation and then in conductivity behavior.

For the lowest temperature values in the range considered, charge relaxation time is quite similar to the times that characterize the transition from d.c. to a.c. regime. In the higher temperature range, free carriers relaxation time is greater than the regime transition time, which may also contribute to the decrease in hopping correlation, as carriers cannot follow processes associated with a.c. regime, which have lower characteristic times.

Kinetics of chain motions at these temperatures follow Arrhenius law as there are no volume restrictions and the presence of regions with larger free volume and enhanced local rotational motions in regularly spaced locations associated with the difference in activation energy.

ACKNOWLEDGMENTS

MM thanks the Agència de Gestió d'Ajuts Universitaris i de Recerca de la Generalitat de Catalunya for financial support (2009SGR1168).

REFERENCES

- [1] Guarrotxena, N.; Schue, F.; Collet, A.; Millán, J. *Polym. Int.* 2003, 52:420-428.
- [2] Guarrotxena, N.; Martínez, G.; Millán, J. *J. Polym. Sci. Polym. Chem.* 1996;34:2387-2397.
- [3] Guarrotxena, N.; Martínez, G.; Millán, J. *J. Polym. Sci. Polym. Chem.* 1996;34:2563-2574.
- [4] Guarrotxena, N.; Martínez, G.; Millán, J. *Eur. Polym. J.* 1997;33:1473.
- [5] Guarrotxena, N.; Martínez, G.; Millán, J. *Polymer* 1999, 40:629-636.
- [6] Martínez, G.; García, C.; Guarrotxena, N.; Millán, J. *Polymer* 1999, 40:1507-1514.
- [7] Guarrotxena, N.; Martínez, G.; Millán, J. *Acta Polymerica* 1999, 50:180-186.
- [8] Guarrotxena, N.; Del Val, J. J.; Millán, J. *Polymer Bulletin* 2001, 47:105-111.
- [9] Guarrotxena, N.; Del Val, J. J.; EliceGUI, A.; Millán, J. *J. Polym. Sci. Polym. Phys.* 2004, 42, 2337-2347.

- [10] Del Val, J. J.; Colmenero, J.; Martinez, G.; Millán, J. J. *Polym. Sci. Polym. Physics* 1994, 32, 871-880.
- [11] Guarrotxena, N.; Martinez, G.; Millán, J. *Polymer* 1997, 38, 1857-1864.
- [12] Guarrotxena, N.; Martinez, G.; Millán, J. *Polymer* 2000, 41, 3331-3336.
- [13] Guarrotxena, N.; Vella, N.; Toureille, A.; Millán, J. *Macromol. Chem. Phys.* 1997, 198, 457-469.
- [14] Guarrotxena, N.; Millán, J.; Vella, N.; Toureille, A.; *Polymer* 1997, 38, 4253-4259.
- [15] Guarrotxena, N.; Vella, N.; Toureille, A.; Millán, J. *Polymer* 1998, 39, 3273-3277.
- [16] Guarrotxena, N.; Contreras, J.; Toureille, A.; Millán, J. *Polymer* 1999, 40, 2639-2648.
- [17] Guarrotxena, N.; Toureille, A.; Millán, J. *Macromol. Chem. Phys.* 1998, 199, 81-86.
- [18] Guarrotxena, N.; Millán, J. *Polymer Bulletin* 1997, 39, 639-646.
- [19] Guarrotxena, N.; Millán, J.; Sessler, G.; Hess, G. *Macromol. Rapid Commun.* 2000, 21, 691-696.
- [20] Guarrotxena, N.; Contreras, J.; Martinez, G.; Millán, J. *Polymer Bulletin* 1998, 41, 355-362.
- [21] Guarrotxena, N.; Retes, J.; Agnel, S.; Toureille, A. *J. Polym. Sci. Polym. Physics* 2009, 47, 633-639.
- [22] Moynihan, C. T. *Solid State Ionics* 1998, 105, 175-183.
- [23] Pissis, P.; Kyritsis, A. *Solid State Ionics* 1997, 97, 105-113.
- [24] Macdonald, J. R. *Solid State Ionics* 2002, 150, 263-279.
- [25] Jonscher AK, *Dielectric relaxation in solids*, Chelsea Dielectric Press, London, 1983.
- [26] Jonscher, A. K. *Universal Relaxation Law*, Chelsea Dielectric Press, London, 1996.
- [27] Sidebottom, D. L.; Green, P. F.; Brow, R. K. *Phys. Rev. Lett.* 1995, 74, 5068-5071.
- [28] Sidebottom, D. L.; Green, P. F.; Brow, R. K. *Phys. Rev. B* 1997, 56, 170-177.
- [29] León, C.; Lucía, M. L.; Santamaría, J. *Phys. Rev. B* 1997, 55, 882-887.
- [30] León, C.; Lucía, M. L.; Santamaría, J.; Sánchez-Quesada, F. *Phys. Rev. B* 1998, 57, 41-44.
- [31] Kalgaonkar, R. A.; Jog, J. P. *Polym. Int.* 2008, 57, 114-123.
- [32] Sengwa, R. J.; Choudhary, S.; Sankhla, S. *Polym. Int.* 2009, 58, 781-789.
- [33] Mahmoud, W. E.; Al-Ghamdi, A. A. *Polym. Int.* 2010, 59, 1282-1288.
- [34] Jonscher, A. K. *Phys. Thin Films* 1980, 11, 222-232.
- [35] Almond, D. P.; West, A. R.; Grant, R. J. *Solid Stat. Comm.* 1982, 44, 1277-1280.
- [36] Ngai, K. L. *Comments of Solid State Physics* 1979, 9, 127-140.
- [37] Ngai, K. *Comments of Solid State Physics* 1979, 9, 141-155.
- [38] Bovey, F. A. *High Resolution NMR of Macromolecules*; Academic Press, New York-London, 1972.
- [39] Laredo, E.; Suarez, N.; Bello, A.; de Gáscue, B. R.; Gómez, M. A.; Fatou, J. M. G. *Polymer* 1999, 40, 6405-6416.
- [40] Grimau, M.; Laredo, E.; Bello, A.; Suarez, N. *J. Polym. Sci. Polym. Phys.* 1997, 35, 2483-2493.
- [41] Bello, A.; Laredo, E.; Grimau, M. *Phys. Rev. B.* 1999, 60, 12764-12774.
- [42] Hatada, K.; Kitayma, T. *NMR Spectroscopy of Polymers*, Chapter 3, Springer-Verlag, 2004.
- [43] Sidebottom, D. L.; Green, P. F.; Brow, R. K. *J. Non-Cryst. Solids* 1995, 183, 151-160.
- [44] Koenig, J. L.; Antoon, M. K. *J. Polym. Sci. Polym. Phys.* 1977, 15, 1379-1395.